YMTHE, Volume *28*

Supplemental Information

Genetically Engineered Cell-Derived Nanoparticles for Targeted Breast Cancer Immunotherapy

Xiaojing Shi, Qinqin Cheng, Tianling Hou, Menglu Han, Goar Smbatyan, Julie E. Lang, Alan L. Epstein, Heinz-Josef Lenz, and Yong Zhang

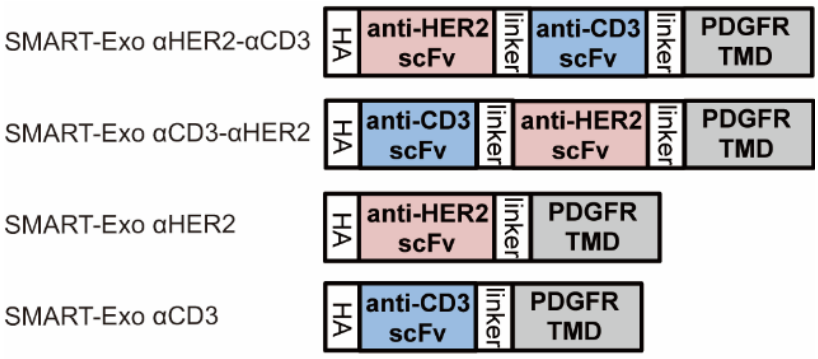

Figure S1. Molecular designs of scFv antibody-PDGFR TMD fusions for the generation of SMART-Exos. Each fusion protein contained an N-terminal HA epitope tag and flexible linkers.

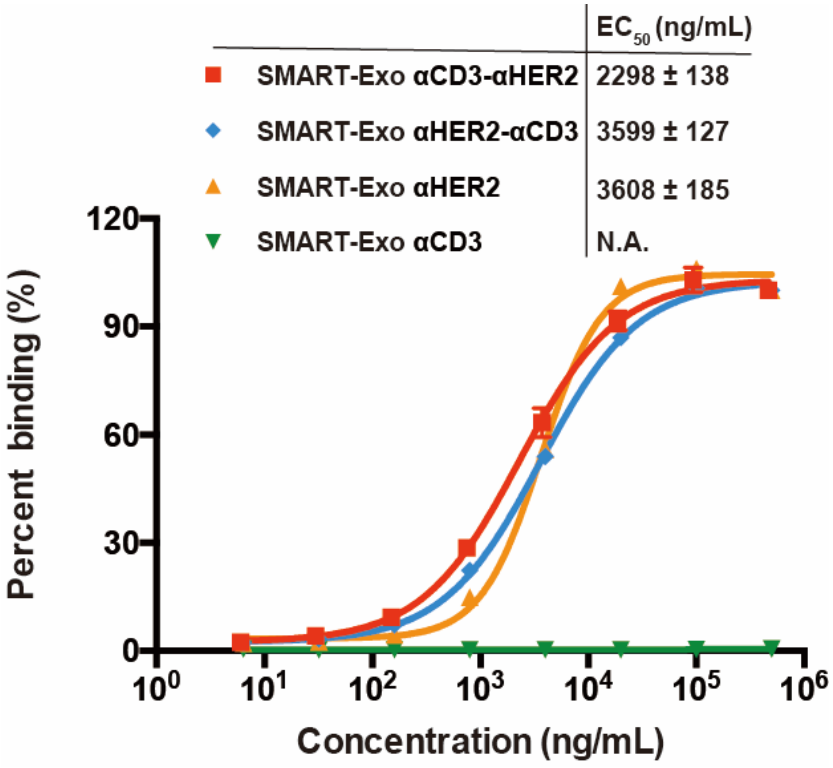

Figure S2. ELISA analysis of binding of the SMART-Exos to human HER2. Human HER2-Fc (2.5 μg/mL) was coated on plates overnight for ELISA analysis. Data are shown as mean ± SD of duplicates.

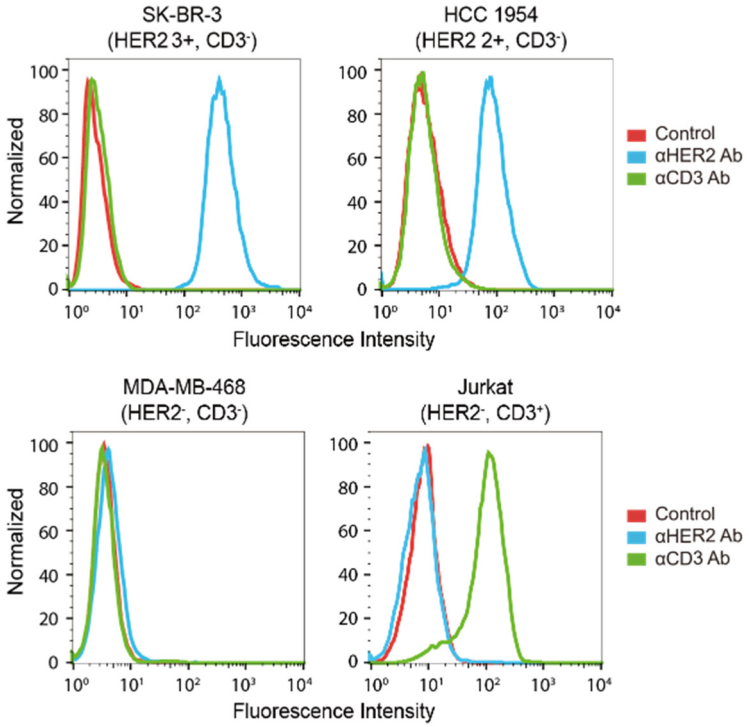

Figure S3. Flow cytometric analysis of HER2 and CD3 expressions of SK-BR-3, HCC 1954, MDA-MB-468, and Jurkat cells. Equal numbers of cells were incubated with the trastuzumab followed by the anti-human IgG Fc-FITC antibody or with the anti-CD3-FITC antibody in PBS with 2% FBS at 4°C for 1 hour.

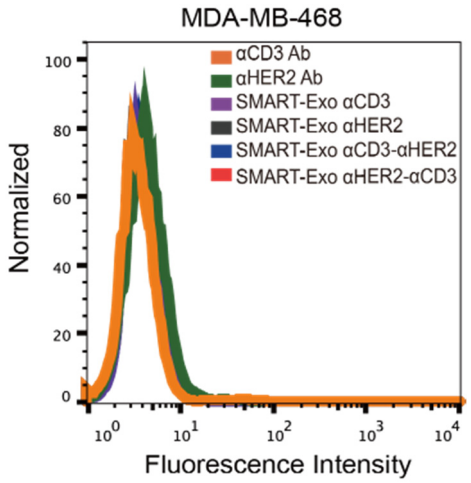

Figure S4. Flow cytometric analysis of SMART-Exos binding to HER2-negative cell line MDA-MB-468. Cells were incubated with 0.1 mg mL^{-1} exosomes on ice, and then stained with the anti-HA antibody and Alexa Fluor 488-conjugated anti-mouse IgG secondary antibody.

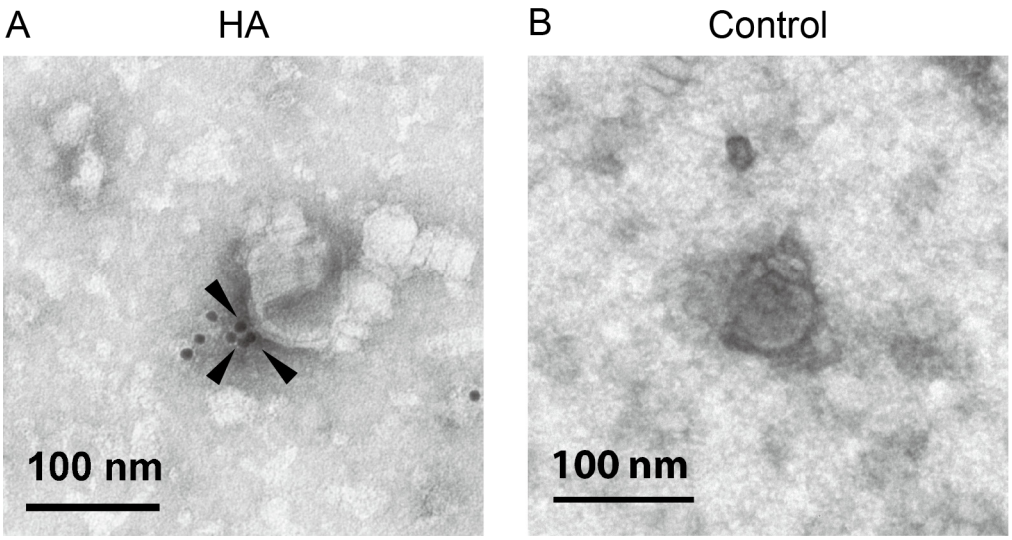

Figure S5. TEM images of the αCD3-αHER2 SMART-Exos showing immunogold labeling of surface HA tags. The αCD3-αHER2 SMART-Exos were stained with the anti-HA antibody (A) or the IgG control antibody (B) as described in Materials and Methods. Arrows indicate gold particles. Scale bars: 100 nm.

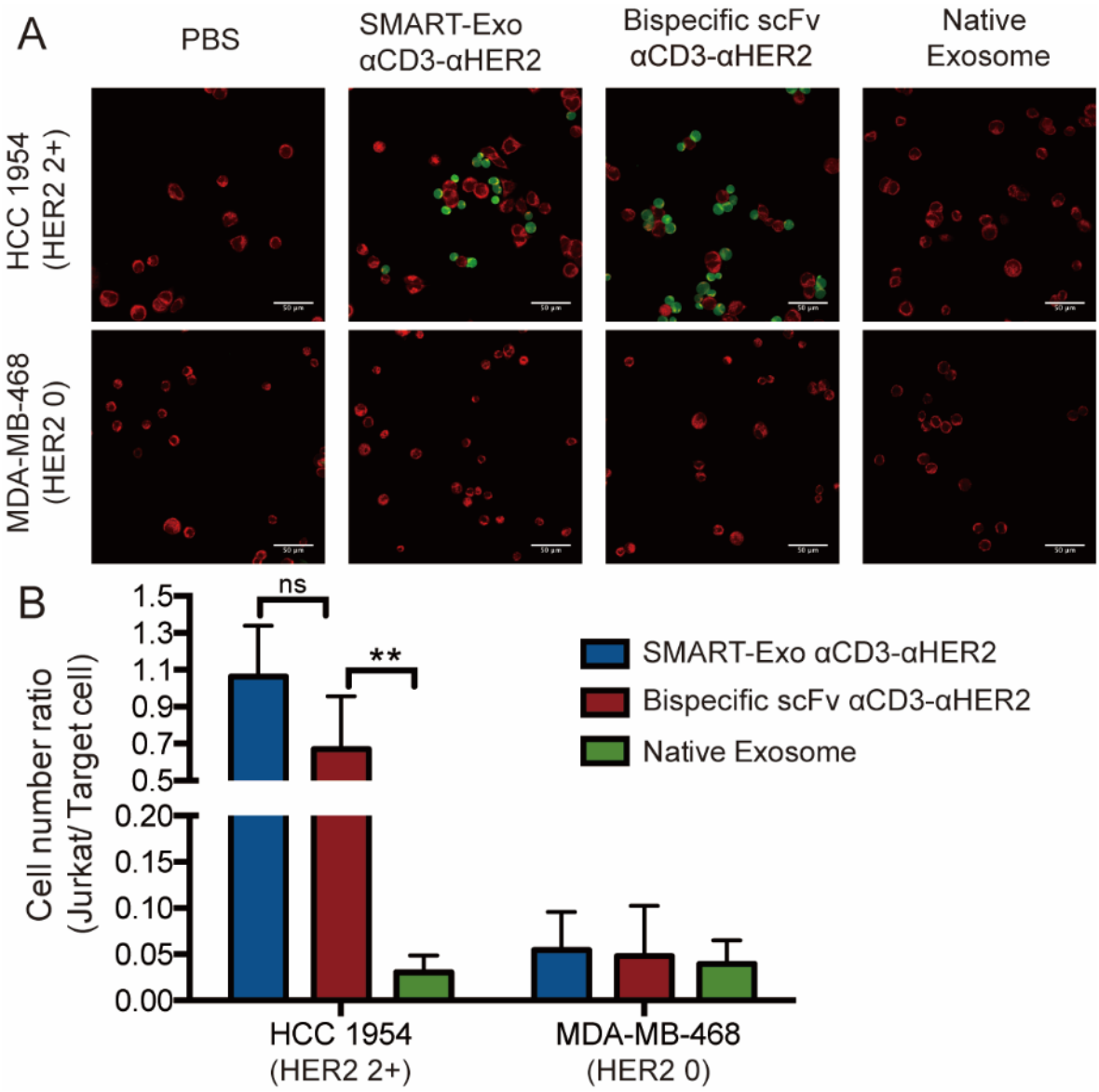

Figure S6. Confocal microscopy of cell-cell crosslinking mediated by αCD3-αHER2 SMART-Exos and bispecific scFv. (A) Crosslinking of HCC 1954 (red) and Jurkat cells (green) (upper panel) and MDA-MB-468 (red) and Jurkat cells (green) (lower panel) mediated by αCD3-αHER2 SMART-Exos and bispecific scFv. PBS and native exosomes were included as controls. Scale bars: 50 μm. (B) Quantitative analysis of confocal microscopy of cell-cell crosslinking induced by SMART-Exos and bispecific scFv. Based on fluorescence color, cell numbers of each cell line were counted to calculate cell number ratios (Jurkat cell:target breast cancer cell) for each treatment group. Data are shown as mean ± SD. (** $P < 0.01$, ns = not significant, $P > 0.05$)

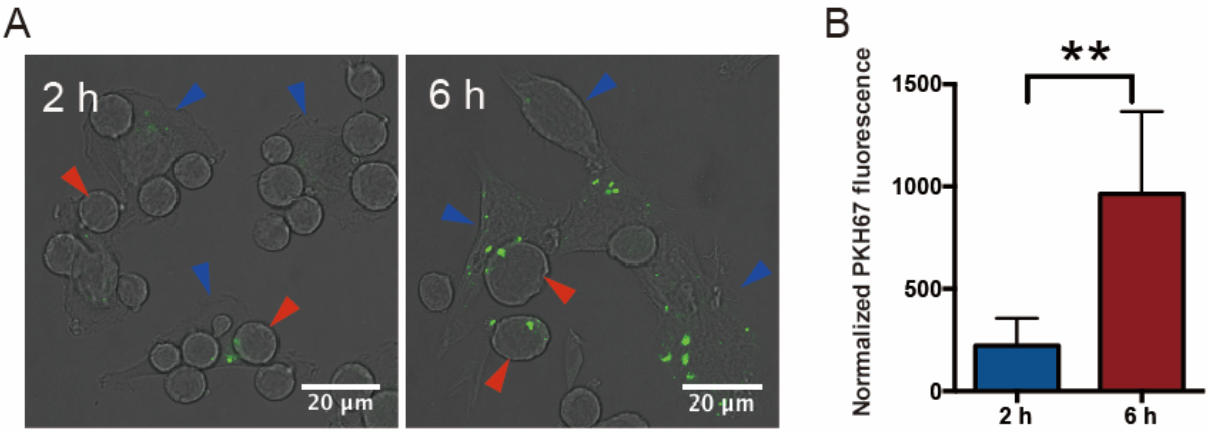

Figure S7. Confocal microscopic analysis of internalization of αCD3-αHER2 SMART-Exos. (A) Confocal imaging of PKH67-labeled αCD3-αHER2 SMART-Exos (green) crosslinking HCC 1954 cells (blue arrow) and Jurkat cells (red arrow) and cellular internalization of PKH67-labeled αCD3-αHER2 SMART-Exos (green) after 2 hours and 6 hours of treatments. Scale bars: 20 µm. (B) Quantification of the internalization of PKH67-labeled αCD3-αHER2 SMART-Exos. PKH67 fluorescence intensities of confocal images are measured and normalized to cell numbers for indicating the amount of internalized αCD3-αHER2 SMART-Exos per cell. Data are shown as mean ± SD. (** $P < 0.01$).

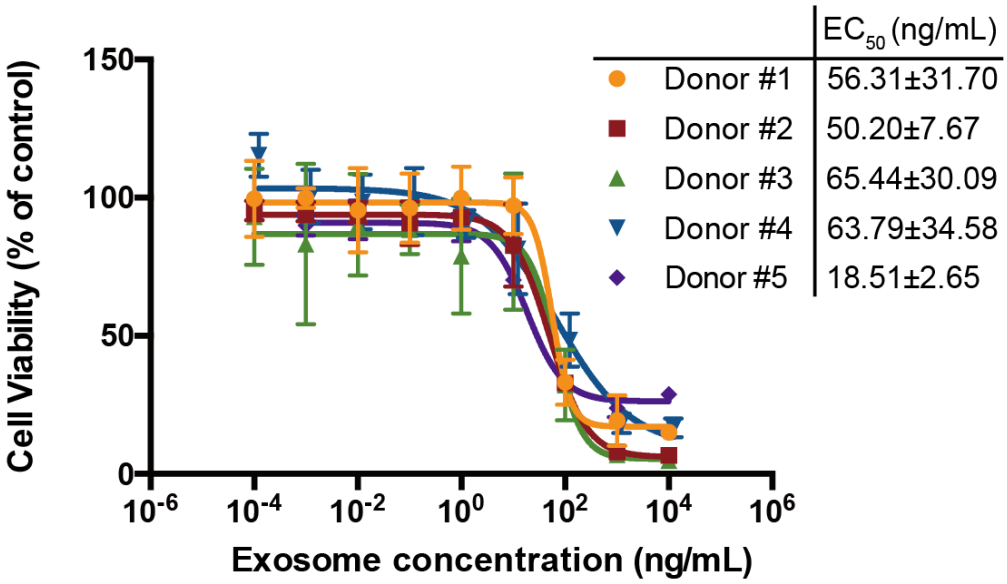

Figure S8. *In vitro* cytotoxicity of αCD3-αHER2 SMART-Exos for HCC 1954 cells (HER2 2+). Non-activated human PBMCs (effector cells) from five different healthy donors were incubated with HCC1954 cells (target cells) at an E:T ratio of 10 for 48 hours in the presence of αCD3-αHER2 SMART-Exos. Following removal of human PBMCs suspensions, viabilities of target cells were determined with MTT assays. Data are shown as mean ± SD of triplicates.

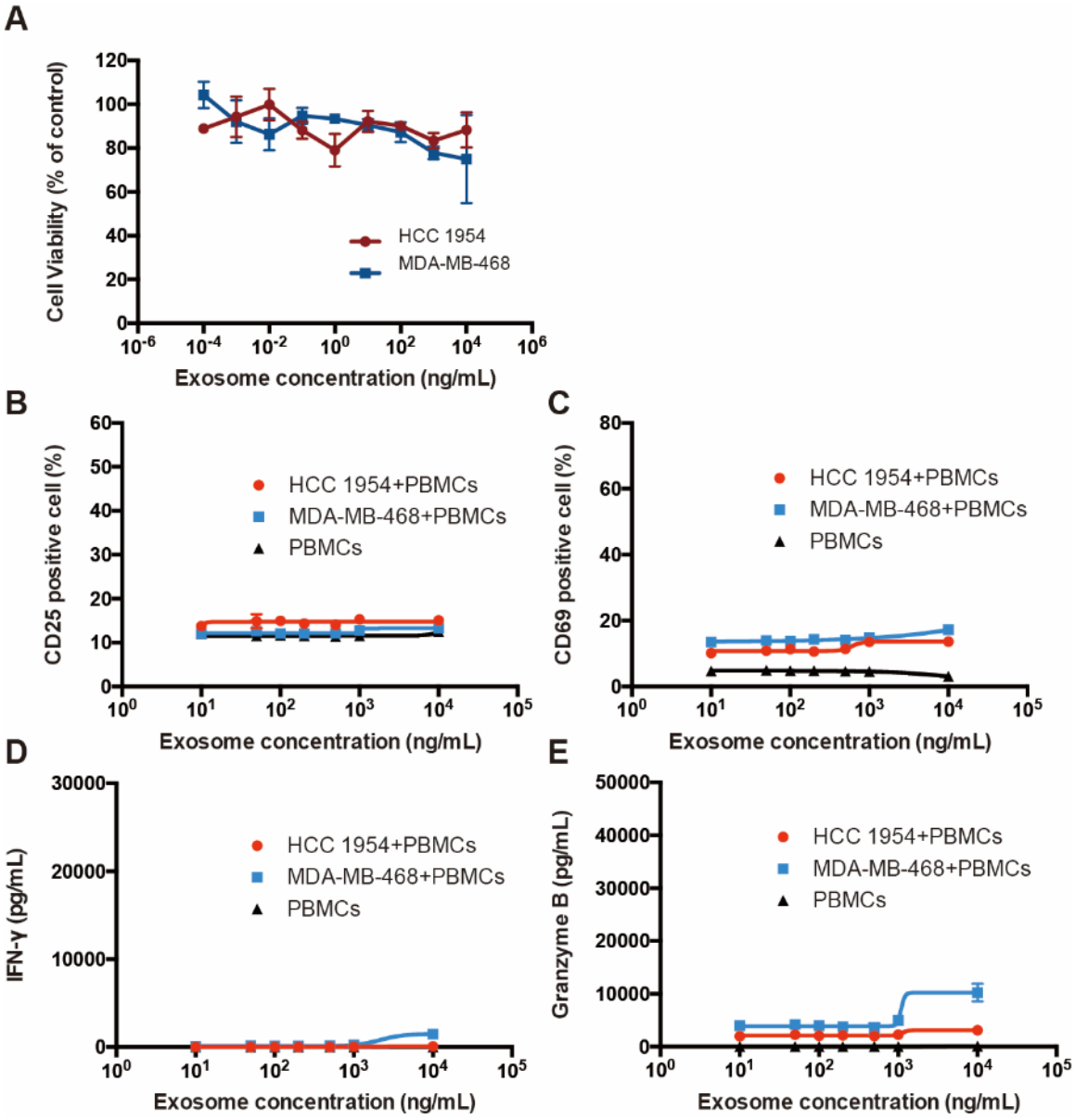

Figure S9. *In vitro* cytotoxicity of native exosomes and effects of native exosomes on T-cell activation. (A) Cytotoxicity of native exosomes for HCC 1954 (HER2 2+) and MDA-MB-468 (HER2 0) cells. Non-activated human PBMCs (effector cells) were incubated with breast cancer cells (target cells) at an E:T ratio of 10 for 48 hours in the presence of native exosomes at various concentrations. Following removal of human PBMCs suspensions, viabilities of target cells were determined with MTT assays. Data are shown as mean ± SD of triplicates. (B)-(E) Effects of native exosomes on T-cell activation at various concentrations. Non-activated human PBMCs were incubated with native exosomes in the presence or absence of MDA-MB-468 or HCC 1954 cells at an E:T ratio of 10 for 24 hours. The percentages of $CD69^+$ and $CD25^+$ T cells were analyzed by flow cytometry. The levels of secreted IFN-γ cytokine and granzyme B were measured by ELISA. Data are shown as mean ± SD of duplicates.

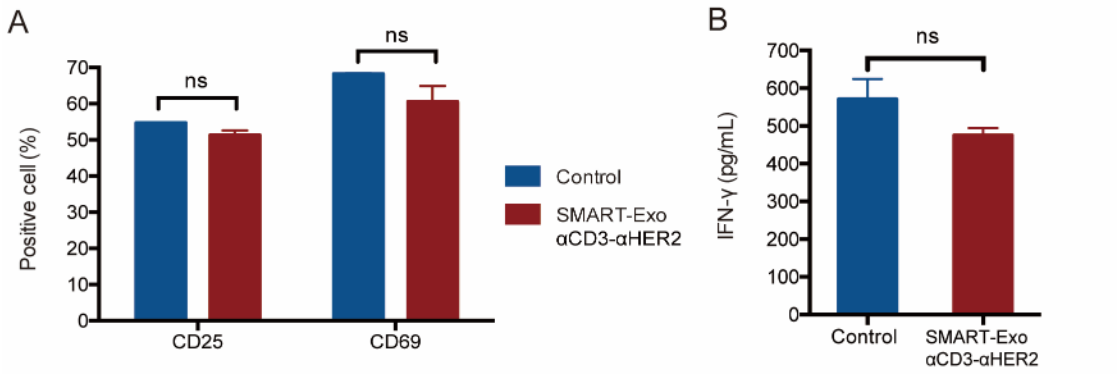

Figure S10. The effects of αCD3-αHER2 SMART-Exos pre-treatment on T cell activation. Non-activated human PBMCs were pre-incubated with αCD3-αHER2 SMART-Exos (200 ng/mL) or PBS (control) for 2 hours at 37°C, followed by washing, resuspension in culture media, and activation with coated αCD3 antibody (clone: OKT3) and soluble αCD28 antibody (clone: 28.2) for 24 hours. (A) The percentages of $CD25^+$ and $CD69^+$ T cells as analyzed by flow cytometry. (B) The levels of secreted IFN-γ cytokine as measured by ELISA. Data are shown as mean ± SD of duplicates. (ns = not significant, $P > 0.05$).

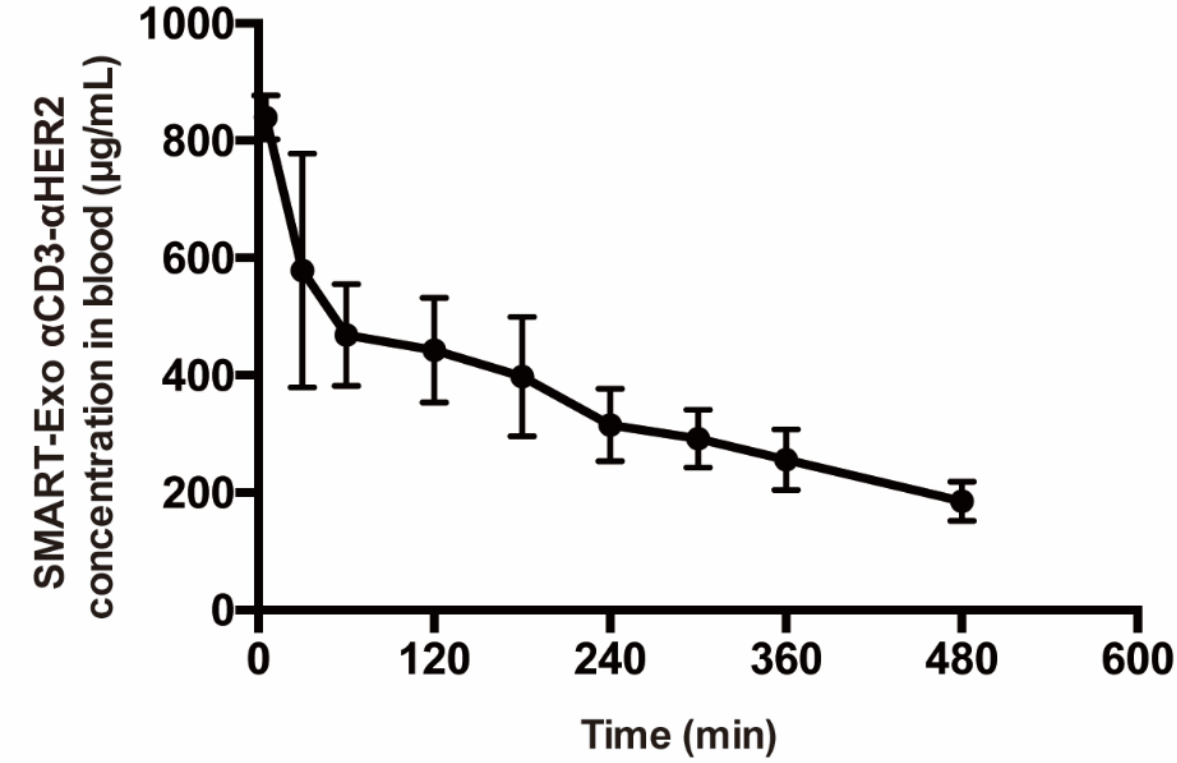

Figure S11. Pharmacokinetics of αCD3-αHER2 SMART-Exos in mice. Plasma concentrations of SMART-Exos were determined by sandwich ELISA post i.v. injection of αCD3-αHER2 SMART-Exos. Data are shown as mean ± SEM (n = 4). The $t_{1/2}$ of αCD3-αHER2 SMART-Exos is 417.03 ± 126.63 min.

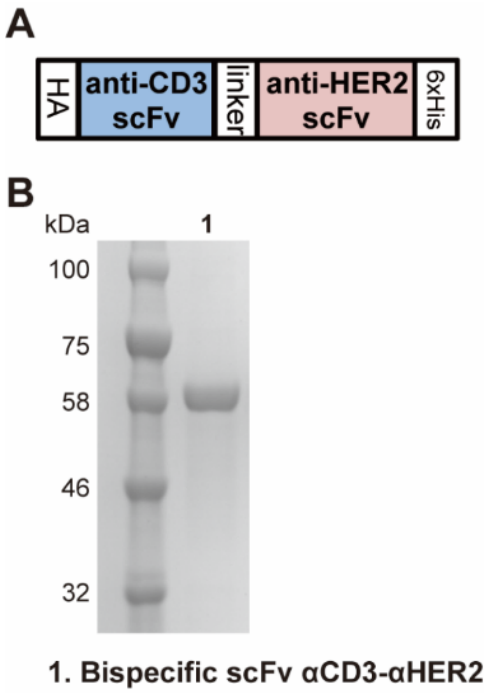

Figure S12. Generation of bispecific scFv αCD3-αHER2 antibody. (A) Molecular design of the bispecific scFv αCD3-αHER2 antibody. The bispecific scFv αCD3-αHER2 antibody contained an N-terminal HA epitope tag, a flexible linker with a sequence identical to that of SMART-Exos αCD3-αHER2, and a C-terminal 6XHis tag. (B) SDS-PAGE gel of the purified bispecific scFv αCD3-αHER2 antibody.

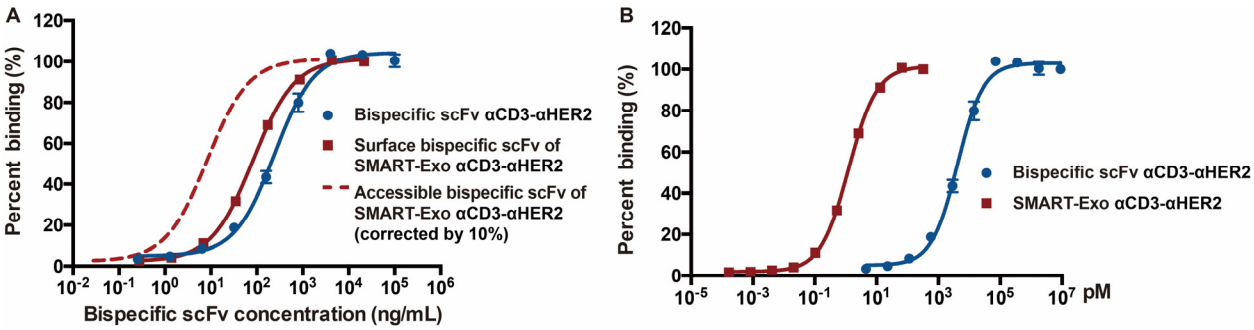

Figure S13. Binding affinities of αCD3-αHER2 SMART-Exos and bispecific αCD3-αHER2 scFv antibody to immobilized human HER2-Fc as measured by ELISA. Recombinant human HER2-Fc was coated on ELISA plates. Following the blocking step, various concentrations of αCD3-αHER2 SMART-Exos and bispecific αCD3-αHER2 scFv antibody were added and incubated. Bound SMART-Exos and bispecific scFv molecules were detected by an anti-HA antibody. (A) Binding affinities based on concentrations of bispecific scFv. The concentrations of surface bispecific scFv of SMART-Exos were determined through ELISA using an anti-HA antibody and serially diluted bispecific αCD3-αHER2 scFv as standards. Considering the average sizes of SMART-Exos (~100 nm in diameter) and immobilized HER2-Fc (~10 nm in diameter), it is estimated that up to 10% of surface displayed bispecific scFv molecules on SMART-Exos are able to participate in binding to the coated HER-Fc. By correcting the accessible bispecific scFv concentrations of SMART-Exos by 10%, the binding curve (broken line) for SMART-Exos was plotted. EC_{50}: 241.5 ± 21.9 ng/mL for free bispecific αCD3-αHER2 scFv; 83.1 ± 2.9 ng/mL for surface bispecific scFv of SMART-Exos; 8.3 ± 0.3 ng/mL for accessible bispecific scFv of SMART-Exos. (B) Binding affinities based on molar concentrations. The molar concentrations of SMART-Exos were calculated based on particle concentrations determined by NTA. EC_{50}: 4160 ± 364 pM for bispecific αCD3-αHER2 scFv; 1.243 ± 0.036 pM for αCD3-αHER2 SMART-Exos. Data are shown as mean ± SD of duplicates.

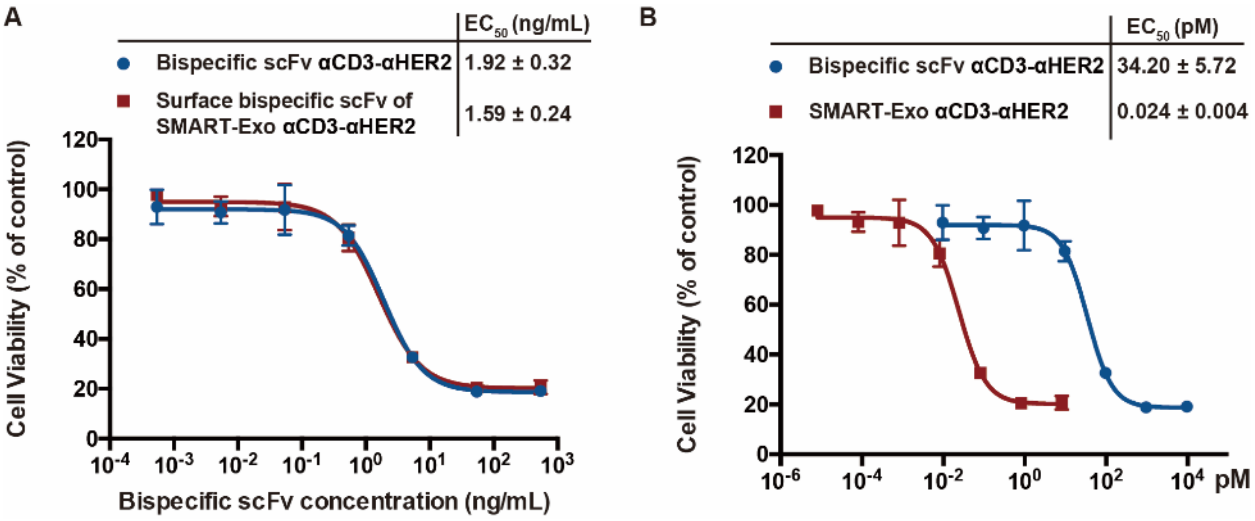

Figure S14. *In vitro* cytotoxicity of αCD3-αHER2 SMART-Exos and bispecific αCD3-αHER2 scFv antibody. Non-activated human PBMCs (effector cells) were incubated with HCC 1954 cells (HER2 2+) (target cells) at an E:T ratio of 10 for 48 hours in the presence of various concentrations of αCD3-αHER2 SMART-Exos or αCD3-αHER2 scFv antibody. Following removal of human PBMCs suspensions, viabilities of target cells were determined with MTT assays. (A) *In vitro* cytotoxicities based on concentrations of bispecific scFv. The concentrations of surface bispecific scFv of SMART-Exos were determined through ELISA using an anti-HA antibody and serially diluted bispecific αCD3-αHER2 scFv as standards. (B) *In vitro* cytotoxicities based on molar concentrations. The molar concentrations of SMART-Exos were calculated based on particle concentrations determined by NTA. Data are shown as mean ± SD of triplicates.

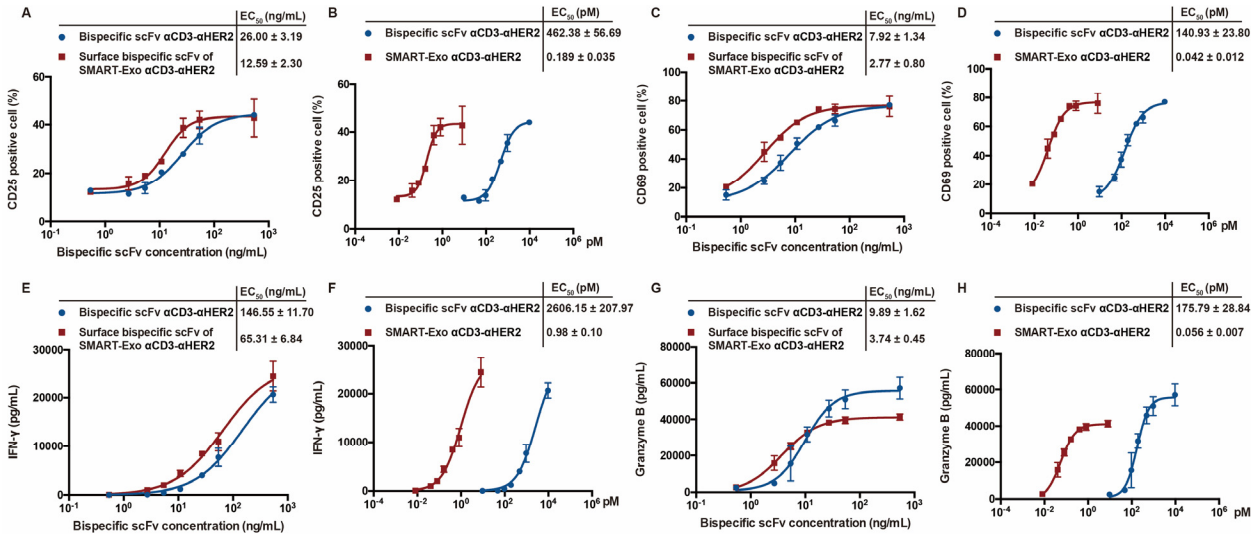

Figure S15. T-cell activation induced by αCD3-αHER2 SMART-Exos and bispecific αCD3-αHER2 scFv antibody. Non-activated human PBMCs were incubated with αCD3-αHER2 SMART-Exos or bispecific αCD3-αHER2 scFv antibody in the presence of HCC 1954 ($HER2^+$) cells at an E:T ratio of 10 for 24 hours. The percentages of $CD25^+$ and $CD69^+$ T cells were analyzed by flow cytometry. The levels of secreted IFN-γ and granzyme B were measured by ELISA. (A), (C), (E), and (G) T-cell activation based on concentrations of bispecific scFv. The concentrations of surface bispecific scFv of SMART-Exos were determined through ELISA using an anti-HA antibody and serially diluted bispecific αCD3-αHER2 scFv as standards. (B), (D), (F), and (H) T-cell activation based on molar concentrations. The molar concentrations of SMART-Exos were calculated based on particle concentrations determined by NTA. Data are shown as mean ± SD of duplicates.

Table S1. List of primers used for molecular cloning.

SMART-Exo αCD3	
BglII-F	GGCCAGATCTGATATCCAGATGACACAGACAACCTCAAGTCTTAG
SalI-R	TTCGTCGACGCTTCCGCCACCCCCGCTGCTAACGGTAACGGTGGTACC
SMART-Exo αHER2	
BglII-F	GCCAGATCTGACATCCAGATGACCCAG
SalI-R	GTTCGTCGACGCTTCCGCCACCCCCAGAGGACACTGTGACCAGGGTGCC
SMART-Exo αHER2-αCD3	
BglII-F	GCCAGATCTGACATCCAGATGACCCAGTCTCCATCC
SalI-R	TTCGTCGACGCTTCCGCCACCCCCGCTGCTAACGGTAACGGTGGTACC
Overlap-F	GGCACCCTGGTCACAGTGTCCTCTGGCGGTGGCGGATCAGGCGGGGGAGGC
Overlap-R	GACTTGAGGTTGTCTGTGTCATCTGGATATCGCTGCCACCTCCGCCTGAGCCTCCCCCGCCTGATCCG
SMART-Exo αCD3-αHER2	
BglII-F	GGCCAGATCTGATATCCAGATGACACAGACAACCTCAAGTCTTAG
SalI-R	GTTCGTCGACGCTTCCGCCACCCCCAGAGGACACTGTGACCAGGGTG
Overlap-F	CAGGCGGGGGAGGCTCAGGCGGAGGTGGCAGCGACATCCAGATGACCCAGTCTCCATCC
Overlap-R	CCTGAGCCTCCCCCGCCTGATCCGCCACCGCCGCTGCTAACGGTAACGGTGGTACC
Bispecific scFv αCD3-αHER2 antibody	
Forward	CACGAATTCGTATCCATATGATGTTCCAGATTATGCTGGGG
Reverse	CCAGCTAGCACTTATCAATGGTGGTGGTGATGGTGAGAGGACACTGTGACCAGGGTG